IARJSET

ISSN (Online) 2393-8021
ISSN (Print) 2394-1588

International Advanced Research Journal in Science, Engineering and Technology

SITES

Smart And Innovative Technologies In Engineering And Sciences

Gyan Ganga College of Technology

Vol. 3, Special Issue 4, November 2016

Heading of Rivet Shape Head from Cylindrical Porous Aluminum-Copper Composites at Different Strain Rates during Cold Forging

Dr. Shrikant Jain[1], Dr. R. K. Ranjan[2], Dr. Surendra Kumar[3]

Professor, Department of Mech. Engineering, GGITS, Jabalpur, India [1]

Principal & Professor, Department of Mech. Engineering, GGCT, Jabalpur, India [2]

Dean R & D, GLA University Mathura, India[3]

Abstract: The paper presents an investigation into the heading of rivet shape head form aluminum-copper porous cylindrical composite specimen clamped at one of its ends, at different strain rates (based on ram velocity) during cold forging under lubricated end conditions. The composites of different compositions were prepared and forged into rivets at different ram velocities: 1.5, 50, 100 and 150 mm/min. The forgeability of all the porous composites into rivet shape head was observed. The yield criterion as proposed by Tabata and Masaki, composite friction law, an appropriate velocity field, a mathematical model considering 'Upper Bound' analysis was developed for relative average forging pressure on the platen during cold forging of the aluminum-copper porous composites into rivet at different ram velocities. Theoretical results have been presented graphically showing the variation of the relative average forging pressure versus percent reduction in height of the porous composites. The required ram travel has also been ascertained. Theoretical and experimentally obtained values of relative average forging pressure versus percent reduction in height were plotted for different composite- specimen and a good correlation was observed. Strain rate effect on forging load during circular rivet head forming process versus percentage reduction in height were presented graphically, analyzed and discussed critically.

Keywords: Al-Cu porous composite, strain rate, yield criterion, interfacial friction law, forgeability**.**

I. INTRODUCTION

Composite metal powder specimen forging has the advantages associated with conventional powder metallurgical processes along with additional strength provided by the elimination of porosity, had been discussed by Cull (1970). Jha and Kumar (1988) investigated the influence of powder particle sizes, compacting pressures, sintering temperatures, and forging parameters on relative density of the specimen along with the deformation characteristics and fracture mechanisms during the cold forging of sintered iron powder specimen under axis-symmetric conditions.

Chitkara and Bhutta (2001) in their investigation showed that in dynamic shape heading of triangular, hexagonal, and octagonal shaped heads from solid cylindrical aluminum specimens, the dynamic die loads were 20- 40 % higher than the static loading. Singh and Jha (2001) have analyzed the dynamic effects during high speed forging of sintered preforms by energy method for axisymmetric and plain strain conditions. They have shown that die velocity has significant effect on deformation characteristics. Ranjan and Kumar (2004) presented a generalized solution to determine die pressure for high speed forging of N-sided polygonal sintered powder disc. Ranjan and Kumar (2004) had also used an upper bound approach to determine the die pressure in closed die forging of hexagonal preform and found the die pressure was minimum for certain dimensional ratios of the preform. Sumathi and Selvakumar (2012) have investigated the workability of sintered copper-silicon carbide preforms during cold axial upsetting. They showed that strength property is very high at 5 % of SiC with copper and the initiation of crack appeared at a low axial strain with higher value of SiC addition. Verma et.al (2013) have investigated the deformation characteristics during open-die forging of silicon carbide particulate reinforced aluminum metal matrix composites (Si-Cp AMC) at cold conditions. Jain S et.al (2015) has investigated the deformation characteristics of polygonal in specific square porous aluminum-copper composites at different strain rates during cold forging. Authors have not yet come across the investigations in which the effect of strain rate (based on ram velocity) on the forging of porous composite specimen, as the strain rate is one of the most important parameter in forging process.

The paper presents an investigation into the heading of rivet shape head form aluminum-copper porous cylindrical composite specimen clamped at one of its ends, at different strain rates (based on ram velocity) during cold

IARJSET
ISSN (Online) 2393-8021
ISSN (Print) 2394-1588
International Advanced Research Journal in Science, Engineering and Technology
SITES
Smart And Innovative Technologies In Engineering And Sciences
Gyan Ganga College of Technology
Vol. 3, Special Issue 4, November 2016

forging under lubricated end conditions. A mathematical model has been developed showing the relative average forging pressure on the platen versus percentage reduction in height during head forming process & required ram travel during cold forging at different ram velocities. The appropriateness of obtained theoretical results has been verified experimentally.

II. BASIC EQUATIONS

An easy way to comply with the conference paper formatting requirements is to use this document as a template and simply type your text into it.

2.1Yield criterion during plastic deformation of porous composite

Basic assumptions:

- The material is isotropic rigid plastic but compressible with volume inconsistency.
- The density distribution is non-uniform throughout the deforming process.
- Yielding is sensitive to hydrostatic stress.
- Deformation is inhomogeneous and barreling is considered.
- Coefficient of friction is constant, and both sliding and sticking friction are considered. The friction due to adhesion (sticking friction) is a function of relative density ρ_r.
- Forging die-faces are flat and rigid.
- Pressure is normal to the contact-surfaces.
- Elastic deformation is neglected.

Tabata and Masaki (1978) proposed yield criterion;

$$\rho^k \sigma_o = \sqrt{3J_2'} \pm 3\eta\sigma_m \qquad (1)$$

where negative sign is for compressive load and $\eta \leq 0$, η and k were determined experimentally:

$$\eta = 0.54(1-\rho)^{1.2}\text{ , k = 2,for } \sigma_m \leq 0 \qquad (2)$$

For axisymmetric conditions the equation (1) becomes

$$\sigma_1 = \frac{\rho^k \sigma_o}{(1-2\eta)} + \frac{(1+\eta)}{(1-2\eta)}\sigma_2 \qquad (3)$$

The moment yielding starts, the equation reduces to give flow stress

$$\lambda = \frac{\rho^k \sigma_o}{(1-2\eta)} \qquad (4)$$

According to Tabata and Masaki (1978) the principal strain increments are:

$$d\varepsilon_i = d\lambda\left[\frac{3(\sigma_i-\sigma_m)}{2\sqrt{3J_2'}} \pm \eta\right], \quad \text{(for i = 1, 2, 3)} \qquad (5)$$

where

$$d\lambda = \frac{\sqrt{2}}{3}\sqrt{(d\varepsilon_1 - d\varepsilon_2)^2 + (d\varepsilon_2 - d\varepsilon_3)^2 + (d\varepsilon_3 - d\varepsilon_1)^2}$$

is a positive constant, the volumetric strain increment $d\varepsilon_v$ is

$$d\varepsilon_v = d\varepsilon_1 + d\varepsilon_2 + d\varepsilon_3 = \pm 3\eta d\lambda = \pm\mu\sqrt{2}\eta[(d\varepsilon_1 - d\varepsilon 2)2+(d\varepsilon 2-d\varepsilon 3)2+(d\varepsilon 3-d\varepsilon 1)2]12 \qquad (6)$$

For axisymmetric compression the compatibility equation becomes

$$\varepsilon_r = \frac{(2\eta-1)}{2(\eta+1)} ln \frac{h_2}{h_1} \qquad (7)$$

Interfacial friction law

Frictional conditions between deforming tool and work piece in metal forming are of great importance and depend on various factors as discussed by Deryagin (1952). During plastic deformation mechanism of composite friction occurs and the shear stress equation becomes

$$\tau = \mu(p + \rho_0\phi_0) \qquad (8)$$

modified for cylindrical preform as proposed by Rooks (1974)

$$\tau = \mu\left[\bar{p} + \rho_0\phi_0\left(1 - \frac{r_m - r}{nr_0}\right)\right] \qquad (9)$$

sticking radius $r_m = r - \left(\frac{h}{2\mu}\right) ln \frac{1}{\sqrt{3}\mu}$ and constant n>>1.

2.2Forging of rivet head from porous metallic cylindrical composites

2.2.1 Preparation of specimens & forging of rivets

The cylindrical composite specimen were fabricated from aluminum-copper powders, mixed in different proportions on weight percentage basis: 100:00, 95:05, 90:10, and 70:30 on 400 kN UTM at a compaction pressure of 300 MPa using a closed cavity circular die-set of 20 mm diameter as shown in figure 1, and sintered at 500o C in endothermic atmosphere. The composite specimen density was obtained simply by measuring dimensions and weight and the relative density was then obtained. These composite specimens had relative density of 0.9 (approximately) and aspect ratio 1.0.

Figure 1 Die set used to fabricate cylindrical porous composite specimen

The specimen was forged in to a rivet on the forging machine of 400 kN capacity at different ram velocities: 1.5, 50, 100, and 150 mm/min with lubricated end

IARJSET
ISSN (Online) 2393-8021
ISSN (Print) 2394-1588
International Advanced Research Journal in Science, Engineering and Technology
SITES
Smart And Innovative Technologies In Engineering And Sciences
Gyan Ganga College of Technology
Vol. 3, Special Issue 4, November 2016

conditions by using closed rivet forming die set comprising of four components as shown in figure 2. One end of the specimen was clamped at the lower part of the die set. The punch of 30 mm diameter moves in a die component having cavity of 30 mm enclosing the upper part of the clamped specimen. The required travel of the punch theoretically calculated as shown in table 1, is set to form the rivet. Figure 3 shows the arrangement of die components during forging of the rivet on the UTM. Approximately 15 mm height of the specimen was used to form the rivet head of 30 mm diameter and 5 mm head thickness. Figures 4 & 5 show the fabricated rivet from the porous aluminum-copper (95:05) composite specimen. The load with percentage reduction in height was recorded in the UTM computer.

Figure 2 Die set to fabricate circular-head rivet form sintered porous specimen

Figure 3 Fabrication of the rivet on UTM

Figure 4 Forged rivet from Aluminum porous specimen

Figure 5 Forged rivet from Aluminum porous specimen

Figure 6 shows the cylindrical porous specimen in rivet-shape heading process. One end of the cylindrical sintered powder porous specimen is clamped at lower end of the die set. The punch has circular cavity to give the shape of circular rivet of 5 mm head thickness. The punch moves down ward with velocity Uo and lower platen remains stationary. 'Upper Bound' analysis is considered in "near net" shape dynamic heading at different ram velocity. During the axisymmetric shaped heading process, the porous specimen is subdivided into two zones of deformation. In zone 1, this case is similar to the axisymmetric forging of cylindrical porous specimen between two flat platens at different strain rates.

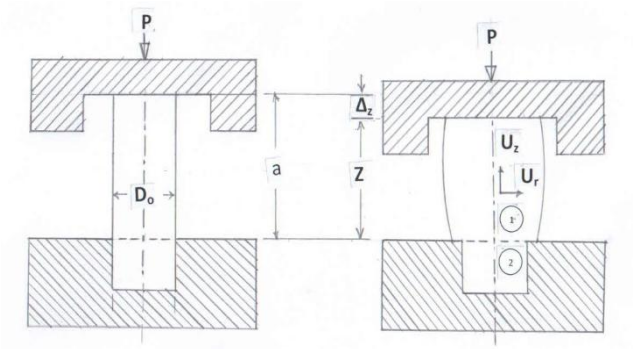

Figure 6 Cylindrical porous composite specimen in rivet shape heading process

2.2.2 Velocity fields and strain rates

Form the traced profile of the compressed porous specimen, velocity field was ascertained which was similar to the velocity field chosen by Chitkara and Bhutta (2001).

$$U_z = -\frac{2U_0 Z}{3a} - \frac{U_0 Z^2}{3a^2}\left\{2 - \frac{Z^2}{a^2}\right\} \quad (10)$$

$$U_\theta = 0 \quad (11)$$

$$U_r = K\left[\frac{U_0 r}{3a} + \frac{2U_0 Zr}{3a^2}\left\{1 - \frac{Z^2}{a^2}\right\}\right] \quad (12)$$

- Strain rates:

$$\dot{\varepsilon_r} = \frac{\partial Ur}{\partial r} = K\left[\frac{U_0}{3a} + \frac{2U_0 Z}{3a^2}\left\{1 - \frac{Z^2}{a^2}\right\}\right] \quad (13)$$

IARJSET
ISSN (Online) 2393-8021
ISSN (Print) 2394-1588
International Advanced Research Journal in Science, Engineering and Technology
SITES
Smart And Innovative Technologies In Engineering And Sciences
Gyan Ganga College of Technology
Vol. 3, Special Issue 4, November 2016

$$\dot{\varepsilon}_\theta = \frac{U_r}{r} + \frac{1}{r}\frac{\partial U_\theta}{\partial \theta} = K\left[\frac{U_0}{3a} + \frac{2U_0 Z}{3a^2}\left\{1 - \frac{Z^2}{a^2}\right\}\right] = \dot{\varepsilon}_r \quad (14)$$

$$\dot{\varepsilon}_z = -2\left[\frac{U_0}{3a} + \frac{2U_0 Z}{3a^2}\left\{1 - \frac{Z^2}{a^2}\right\}\right] \quad (15)$$

Using compressibility equation

$$(\dot{\varepsilon}_r + \dot{\varepsilon}_\theta + \dot{\varepsilon}_z) = \pm 2\eta\sqrt{(\dot{\varepsilon}_r - \dot{\varepsilon}_\theta)^2 + (\dot{\varepsilon}_\theta - \dot{\varepsilon}_z)^2 + (\dot{\varepsilon}_z - \dot{\varepsilon}_r)^2} \quad (16)$$

The value of K for compressive load is

$$K = \frac{(1-2\eta)}{(1+\eta)} \quad (17)$$

• Internal power of deformation (W_i):

$$W_i = \frac{2}{\sqrt{3}}\sigma_0^* \int \sqrt{\frac{1}{2}\dot{\varepsilon}_{ij}\dot{\varepsilon}_{ij}}\, dv \quad \because dv = 2\pi r dr dz \quad (18)$$

$$W_i = \frac{2\pi\sqrt{2}}{\sqrt{3}}\sigma_0^* \iint \sqrt{\left(\dot{\varepsilon_r}^2 + \dot{\varepsilon_\theta}^2 + \dot{\varepsilon_z}^2\right)}\, r dr dz$$

substituting the value of strain rates

$$W_i = \frac{4\pi\sqrt{(K^2+2)}}{\sqrt{3}}\sigma_0^* \int_{r=0}^{r_0}\int_0^a \left[\frac{2U_0}{3a} + \frac{8U_0 Z}{3a^2}\left\{1 - 4Z2a2rdrdz = K2 + 23\pi r02\sigma 0 * U0\right. \quad (19)$$

• Energy dissipation due to velocity discontinuity (W_v):
At Z = a (top) surfaces the velocity discontinuity is

$$|\Delta V| = K\left[\frac{U_0 r}{3a}\right] \quad (20)$$

$$W_v = 2\pi\sigma_0^* \int_0^{r_0} |\Delta V| r dr$$

$$W_v = \frac{2\pi r_0^3 \sigma_0^* U_0 K}{9a} \quad (21)$$

• Frictional power losses (W_f):
At the top and bottom surfaces Z = 0 & Z = a, the velocity discontinuity is: $|\Delta V| = K\left[\frac{U_0 r}{3a}\right]$

The energy dissipation rate due to friction at the tool metal interfaces is given by

$$W_{ft} = 2\pi\left[\int_0^{r_{ex}} K\left|\frac{U_0 r}{3a}\right| + \int_{r_o}^{r_{ex}} K\left|\frac{U_0 r}{3a}\right|\right]\tau|\Delta U| r dr = W_{ft1} + W_{ft2} \quad (22)$$

where rex is new expanded radius of the specimen. Considering composite friction, the sticking zone lies at the centre and in its vicinity and rest of the outer area of contact surface is a sliding zone. The shear stress as given by Rooks (1974):

$$\tau = \mu\left[\bar{p} + \rho_0 \emptyset_0\left(1 - \frac{r_m - r}{n r_0}\right)\right] \quad (23)$$

Sticking radius $r_m = r - \left(\frac{h}{2\mu}\right) ln \frac{1}{\sqrt{3}\mu}$ and n is a constant, n>>1.

At top surface of the rivet head, i.e. z = a, r = 0 to $r = r_{ex}$

$$W_{ft1} = 2\pi \int_0^{r_{ex}} \mu K\left[\bar{p} + \rho_0\varphi_0\left(1 - \frac{r_m - r}{n r_0}\right)\right]\left(\frac{U_0 r}{3a}\right) r dr$$

Putting $\rho_0\varphi_0 = x.p$ & integrating

$$W_{ft1} = \left(\frac{2\pi\mu\bar{p}KU_0}{3a}\right)\left[\frac{r_{ex}^3}{3} + \frac{x.r_{ex}^3}{3} - \frac{x.r_m.r_{ex}^3}{3nr_0} + \frac{x.r_{ex}^4}{4nr_0}\right] \quad (24)$$

Similarly at bottom surface of rivet head i.e. z = 0, r = r_0 to r = r_{ex}

$$W_{ft2} = \left(\frac{2\pi\mu\bar{p}KU_0}{3a}\right)\left[\frac{(r_{ex}^3 - r_0^3)}{3} + \frac{x.(r_{ex}^3 - r_0^3)}{3} - x.rm.(rex3 - r03)3nr0 + x.(rex4 - r04)4nr0\right] \quad (25)$$

total frictional power loss is given by adding the equations 24 & 25.

$$W_{ft} = \frac{2\pi r_0^3 \mu\overline{pK}U_0}{9a}\left[\left(1 + x - \frac{x\, r_m}{n\, r_0}\right)\left\{2\left(\frac{r_{ex}}{r_0}\right)^3 - 1\right\} + 3.xrex4nr02rexr04 - 1\right. \quad (26)$$

Energy dissipation due to Inertia (W_a):

$$W_a = \rho_p \int U_i \dot{U}_i dv \quad (27)$$

ρp - specimen density. The equation in expanded form

$$W_a = 2\pi\rho_p \int_{z=0}^{a}\int_0^{r_0} \{U_r\dot{U}_r + U_\theta\dot{U}_\theta + U_z\dot{U}_z\} r dr\, dz$$

The acceleration-components $\dot{U}_r$, $\dot{U}_\theta$, and $\dot{U}_z$ in the cylindrical coordinate system (r, θ, z) are:

$$\dot{U}_r = \frac{\partial U_r}{\partial t} + U_r\frac{\partial U_r}{\partial r} + \frac{U_\theta}{r}\frac{\partial U_r}{\partial \theta} + U_z\frac{\partial U_r}{\partial z} - \frac{U_0^2}{r}$$

$$\dot{U}_\theta = \frac{\partial U_\theta}{\partial t} + U_r\frac{\partial U_\theta}{\partial r} + \frac{U_\theta}{r}\frac{\partial U_\theta}{\partial \theta} + U_z\frac{\partial U_\theta}{\partial z} + \frac{U_\theta U_r}{r}$$

$$\dot{U}_z = \frac{\partial U_z}{\partial t} + U_r\frac{\partial U_z}{\partial r} + \frac{U_\theta}{r}\frac{\partial U_z}{\partial \theta} + U_z\frac{\partial U_z}{\partial z}$$

substituting the values

$$\dot{U}_\theta = 0 \quad (28)$$

$$\dot{U}_r = K\left[\frac{r}{3a} + \frac{2Zr}{3a^2}\left\{1 - \frac{Z^2}{a^2}\right\}\right]\left[\dot{U} - KU_o^2\left(\frac{1}{3a} + \frac{2Z}{3a^2}\left\{1 - Z2a2 + U02r1 - 2Kr3a21 - Z2a22Z3a + Z23a22 - Z2a2\right.\right.\right. \quad (29)$$

$$\dot{U}_z = -\left[\dot{U} - U_0\left(\frac{2}{3a} + \frac{4z}{3a^2} - \frac{3z^3}{3a^2}\right)\right]\left[\frac{2Z}{3a} + \frac{Z^2}{3a^2}\left(2 - \frac{Z^2}{a^2}\right)\right] \quad (30)$$

substituting the velocity and acceleration components in the equation and after integration

$$W_a = 2\pi r_0^2 U_0\rho_p\left[\dot{U}a\left\{0.213K^2\left(\frac{r_o}{a}\right)^2 + 0.167\right\} + Uo20.0439K2roa2 + K4 + 0.056\right. \quad (31)$$

IARJSET
ISSN (Online) 2393-8021
ISSN (Print) 2394-1588
International Advanced Research Journal in Science, Engineering and Technology
SITES
Smart And Innovative Technologies In Engineering And Sciences
Gyan Ganga College of Technology
Vol. 3, Special Issue 4, November 2016

• External power J^* supplied by the press:

$$J^* = W_i + W_v + W_f + W_a \qquad (32)$$

$$J^* = \int F_i U_0 ds = PU_0 = U_0 \int_0^{r_0} 2\pi r \bar{p} dr = \pi r_0^2 \bar{p} U_0 \qquad (33)$$

$\bar{p}$ is average pressure

$$J^* = \int F_i U_0 ds = \pi r_0^2 \bar{p}\, U_0 = W_i + W_v + W_f + W_a \qquad (34)$$

Substituting the values of Wi, Wv, Wf, & Wa in equation (32),

Relative average forging pressure on the platen:

$$\frac{\bar{p}}{\sigma_0^*} = \frac{\left[\frac{\sqrt{(K^2+2)}}{\sqrt{3}} + \frac{2}{9}\left(\frac{r_0}{a}\right)K + \frac{2\rho_p}{\sigma_0^*}\left[\dot{U}a\left\{0.213K^2\left(\frac{r_0}{a}\right)^2 + 0.167\right\} + U_o{}^2\left\{0.0439K^2\left(\frac{r_0}{a}\right)^2 + \frac{K}{4} + 0.056\right\}\right]\right]}{1 - \frac{2\mu K}{9}\left(\frac{r_0}{a}\right)\left[\left(1 + x - \frac{x\, r_m}{n\, r_0}\right)\left\{2\left(\frac{r_{ex}}{r_0}\right)^3 - 1\right\} + \frac{3.x}{4n}\left(\frac{r_{ex}}{r_0}\right)\left\{2\left(\frac{r_{ex}}{r_0}\right)^4 - 1\right\}\right]} \qquad (35)$$

The dynamic effect is expressed as

$$\zeta = \frac{\left|\frac{p_{av}}{\sigma_o^*}\right|_{with\ dynamic\ \ effect} - \left|\frac{p_{av}}{\sigma_o^*}\right|_{without\ dynamic\ \ effect}}{\left|\frac{p_{av}}{\sigma_o^*}\right|_{with\ dynamic\ \ effect}} \qquad (36)$$

Using the equation 35 for porous aluminum-copper porous specimen the required travel of the punch and forging load during the formation of rivet has been estimated as shown in table 1.

Aluminum cylindrical prefrom upset forging of Rivet at different strain rates:-

Mod of E of Al in Gp	Strain	Stress
70	0.002	105 Main Rate
Rel. D	Eta	Flow gm/min
0.916	0.028	62.17	1.5

A-Relative Density =0.9 and Mue=0.3, x=0.3 & n=3 U=0.0002

$$r_2 = r_1 + r_1\left(\frac{(2\eta - 1)}{2(1+\eta)}\right) ln\left(\frac{h_2}{h_1}\right)$$

Density	Sr.	ρ	$\eta = 0.54(1-\rho)^{12}$	$\frac{(2\eta-1)}{2(1+\eta)}$	K	h(a)	% red	$\frac{h_2}{h_1}$	$ln\frac{h_2}{h_1}$	r_o	r_2	μ	r_m	x	n	$\frac{r_0}{a}$	$\frac{r_{ex}}{r_o}$	$\frac{r_m}{r_o}$	$\frac{x}{n}$	$\left\|\frac{\sigma_z}{\sigma_r}\right\|_m$	$\left\|\frac{\sigma_z}{\sigma_r}\right\|_m$	$\frac{2K}{9}\left(\frac{r_0}{a}\right)$	$\frac{\rho^k}{(1-2\eta)}$ Factor	Gpa	strain %	ρ_p
2700	1	0.9	0.034	-0.45	0.901	15	0	1	0	10	10	0.3	0	0.3	3	0.667	1	0	0.1	0.937	0.968	0.134	0.869	70	0.1	2430
2700	2	0.9	0.034	-0.45	0.901	14	6.667	0.933	-0.07	10	10.31	0.3	0	0.3	3	0.667	1.031	0	0.1	0.937	0.968	0.134	0.869	70	0.1	2430
2700	3	0.9	0.034	-0.45	0.901	13	13.33	0.867	-0.14	10	10.64	0.3	0	0.3	3	0.667	1.064	0	0.1	0.937	0.968	0.134	0.869	70	0.1	2430
2700	4	0.9	0.034	-0.45	0.901	12	20	0.8	-0.22	10	11.01	0.3	0	0.3	3	0.667	1.101	0	0.1	0.937	0.968	0.134	0.869	70	0.1	2430
2700	5	0.9	0.034	-0.45	0.901	11	26.67	0.733	-0.31	10	11.4	0.3	0	0.3	3	0.667	1.14	0	0.1	0.937	0.968	0.134	0.869	70	0.1	2430
2700	6	0.9	0.034	-0.45	0.901	10	33.33	0.667	-0.41	10	11.83	0.3	0	0.3	3	0.667	1.183	0	0.1	0.937	0.968	0.134	0.869	70	0.1	2430
2700	7	0.9	0.034	-0.45	0.901	9	40	0.6	-0.51	10	12.3	0.3	0	0.3	3	0.667	1.23	0	0.1	0.937	0.968	0.134	0.869	70	0.1	2430
2700	8	0.9	0.034	-0.45	0.901	8	46.67	0.533	-0.63	10	12.83	0.3	0	0.3	3	0.667	1.283	0	0.1	0.937	0.968	0.134	0.869	70	0.1	2430
2700	9	0.9	0.034	-0.45	0.901	7	53.33	0.467	-0.76	10	13.43	0.3	0	0.3	3	0.667	1.343	0	0.1	0.937	0.968	0.134	0.869	70	0.1	2430
2700	10	0.9	0.034	-0.45	0.901	6	60	0.4	-0.92	10	14.13	0.3	0	0.3	3	0.667	1.413	0	0.1	0.937	0.968	0.134	0.869	70	0.1	2430
2700	10	0.9	0.034	-0.45	0.901	5	66.67	0.333	-1.1	10	14.95	0.3	0	0.3	3	0.667	1.495	0	0.1	0.937	0.968	0.134	0.869	70	0.1	2430

Table 1 Theoretical estimations of forging load and tool travel during rivet-formation

Parametric Analysis:

The parametric results are presented graphically. The variation of the relative average forging pressure on the forging tool versus percentage reduction in height of the porous specimen have been plotted using the equation (35) by changing one of the considered parameters. Figure 7 shows this variation for different values of ram velocity. It is observed that for given percentage reduction in height as the ram velocity increases the relative average forging pressure also increases. Figure 8 and figure 9 show this variation for different values of coefficient of friction and cohesive friction factor 'x' respectively. For considered percentage reduction in height as these values are increased the relative average forging pressure also increased. Figure 10 shows that with the increase in the value of constant 'n' the relative average forging pressure decreases.

Figure 11 shows the variation of the relative average forging pressure versus ram velocity at 50 percent height reduction for different relative densities of specimen. Figure 12 shows the variations of dynamic effect with ram velocity for different relative densities of specimen. For considered ram velocity, as the relative density increases the relative average forging pressure and the dynamic effect also increases. As the relative density increases the porosity of the specimen reduces resulting in higher relative average forging pressure.

IARJSET

ISSN (Online) 2393-8021
ISSN (Print) 2394-1588

International Advanced Research Journal in Science, Engineering and Technology

SITES

Smart And Innovative Technologies In Engineering And Sciences

Gyan Ganga College of Technology

Vol. 3, Special Issue 4, November 2016

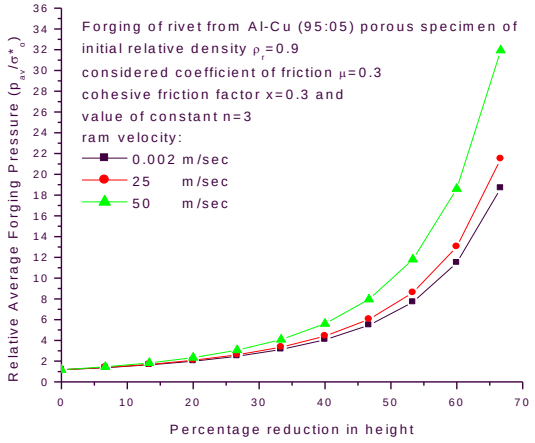

Figure 7 Relative average forging pressure versus percentage reduction in height

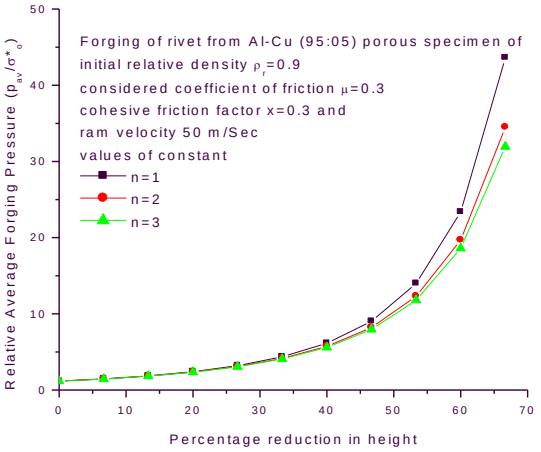

Figure 10 Relative average forging pressure versus percentage reduction in height

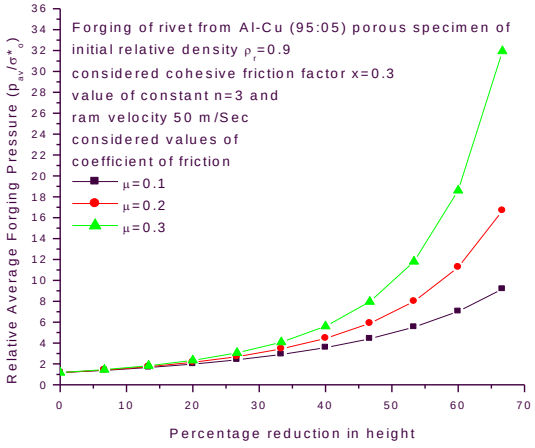

Figure 8 Relative average forging pressure versus percentage reduction in height

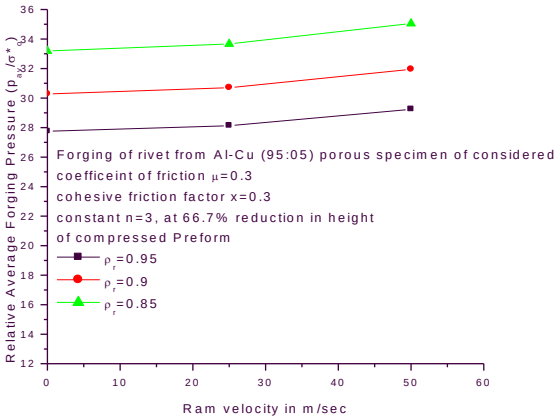

Figure 11 Relative average forging pressure versus ram Velocity

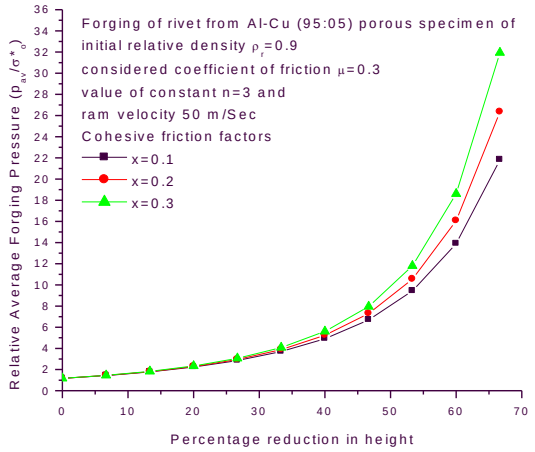

Figure 9 Relative average forging pressure versus percentage reduction in height

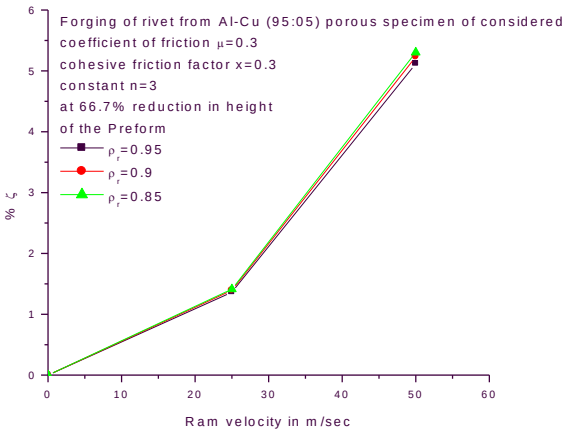

Figure 12 Variation of dynamic effect versus ram velocity

IARJSET
ISSN (Online) 2393-8021
ISSN (Print) 2394-1588
International Advanced Research Journal in Science, Engineering and Technology
SITES
Smart And Innovative Technologies In Engineering And Sciences
Gyan Ganga College of Technology
Vol. 3, Special Issue 4, November 2016

III. EXPERIMENTAL VERIFICATION

The density and modulus of elasticity of composite solid metal were calculated as under:

the density $$\rho_{Alcu} = \left[\frac{100}{\left(\frac{\%\ of\ Al}{\rho_{Al}}\right)+\left(\frac{\%\ of\ Cu}{\rho_{Cu}}\right)}\right]$$

the modulus of elasticity

$$E_{AlCu} = \left[\frac{\left(\frac{\%\ of\ Al}{\rho_{Al}}\right)E_{Al}+\left(\frac{\%\ of\ Cu}{\rho_{Cu}}\right)E_{Cu}}{\left(\frac{\%\ of\ Al}{\rho_{Al}}\right)+\left(\frac{\%\ of\ Cu}{\rho_{Cu}}\right)}\right]$$

The density of aluminum and copper metals were considered as 2.7 gm/cm^3 and 8.94 gm/cm^3 and modulus of elasticity as 70 GPa and 120 GPa respectively. The flow stress "σo" for the composite was calculated at strain value of 0.15%. The composite-preforms of considered aluminum-copper compositions were prepared (relative density 0.9 approximately) and forged at different ram velocities: 1.5, 50, 100 and 150 mm/min. In this paper only the experimental results of the rivet forging form Al-Cu (95:05) composite porous specimen at ram velocity of 1.5 mm/min had been considered. The relative density of the compressed specimen increases with the reduction in height due to forging. The experimentally obtained values were superimposed on the theoretically obtained results using equation 35 with appropriate multiplier and plotted for the variation of the relative average forging pressure versus percent reduction in height as shown in figure 12 for considered coefficient of friction as 0.3, cohesive factor "x" as 0.3 and constant n=3n with different relative densities of specimen as 0.9, 0.95 and 0.98. It is observed that as the forging pressure increases, the compressed preform density increases, which is evident from the experimental curve intersecting the theoretical curves.

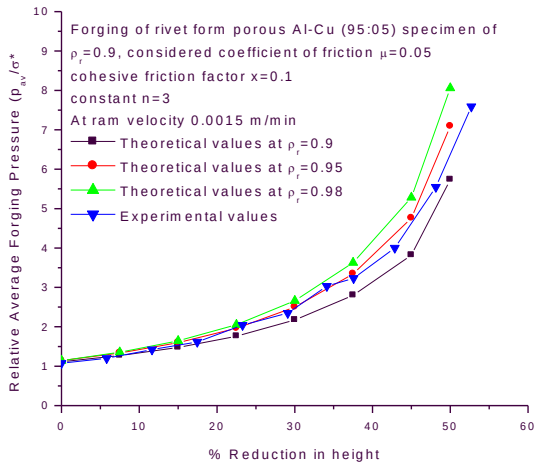

Figure 12 Theoretical and experimental load versus percentage reduction in height

IV. RESULTS AND DISCUSSIONS

The experimental results had been plotted as the variation of the relative average forging pressure versus percentage reduction in height, shown in figure 13, for the specimen of relative density 0.9, forged at ram velocity 2 mm/sec. The experimental values and theoretically obtained values using equation 35 were superimposed for the specimens of relative densities: 0.9, 0.95 and 0.98 and considered values of coefficient of friction 0.3, cohesive factor "x" 0.3 and constant n=3. A close agreement of experimental and theoretical results has been observed. As the forging pressure increases the compressed specimen density also increases, this is evident from the experimental result curve intersecting the theoretical results curves.

Theoretically determined die load and die movement curves are continuous during the process for selected relative densities of the specimens and also experimentally obtained curves are continuous but cutting the theoretical curves of higher relative density of the specimens. At different ram velocity the specimens of similar relative density and for the same die movement, the die loads are about 20-30 % higher in comparison with at ram velocity of 1.5 mm/sec. The cracks on free surface of the rivet show the limit of maximum applied load for making desired dimension of the rivet. For making cracks free rivet one should apply the load below the maximum obtained load. During experimentation the energy consumed in the forming of metal powder specimen is lesser than that of the wrought material. Also the flowability and near-net shape promotes this product/process for commercial use.

During shape head-forging process, the controlling factors are: strain rate (based on ram velocity), the amount of interfacial friction between die-work piece interfaces, the initial density and composition of the specimen. The correlation between experimental and predicted load values based on the upper bound analysis taking inertia into account is considered reasonably satisfactory for these preliminary investigations. There is a need for some further investigation in the dynamic heading analysis, especially at the corner filling stage for the shapes such as triangular, square, hexagonal etc. to obtain good correlation between analytical predictions and experiments.

The developed theory for the relative average forging pressure on the platen during forging of the composite porous specimen at different strain rates (based on ram velocity) did not take in to account the changing relative density of the compressed specimen. The parametric analysis had been done for the variation of one of the parameter keeping other parameters as constant. The experimental results coincide well with the theoretical results in the initial stage of the forging. As the copper

IARJSET
ISSN (Online) 2393-8021
ISSN (Print) 2394-1588
International Advanced Research Journal in Science, Engineering and Technology
SITES
Smart And Innovative Technologies In Engineering And Sciences
Gyan Ganga College of Technology
Vol. 3, Special Issue 4, November 2016

percentage was increasing in the composite specimen, the deformation behavior was changing from ductile to brittle. In fact this is a matter of critical study in powder metallurgy to ascertain at what composition and sintering temperature the deformation behavior change from ductile to brittle of composite specimens.

The forgeability of the composite porous specimens had been considered at the percent reduction in height at which cracks were observed by the naked eyes. For the ram velocities of 1.5, 50, 100 and 150 mm/min, the forgeability of the specimens were observed as for: aluminum specimens at 52, 48, 42, and 38 respectively, aluminum-copper (95:05) composite specimens at 41, 36, 32, and 27 percent respectively, aluminum-copper (90:10) composite specimens at 36, 30, 25, and 23 percent respectively, and aluminum-copper (70:30) composite specimens at 18, 17, 15, and 13 percent respectively. The forgeability was falling with the increase of ram velocity as well as the percent increase in copper proportions in the composite. If heating of the die-set is provided which will certainly result in improving the forgeability. There is scope for further investigation in this direction.

Notations

ρ_r	relative density of the specimen
φ_0	specific cohesion of the contact surface
λ	flow stress of the metal powder specimen
k	constant equal to 2
η	function of relative density of specimen
$d\lambda$	a positive constant
P	die-load
p	pressure
τ	shear stress
n	a constant quantity much greater than unity
μ	Coefficient of friction
$\sigma_1, \sigma_2, \sigma_3$	principal stresses
$d\varepsilon_1, d\varepsilon_2, d\varepsilon_3$,	principal-strain increments
x, y, z	Cartesian co-ordinates
r, θ, z	Polar co-ordinates
a	initial height of the specimen
h	instantaneous thickness of the
σ_0	yield stress of the non-work-hardening composite metal
σ_m	hydrostatic stress
J'_2	second invariant of the deviatoric stress
r_m	radius of the sticking zone

Subscripts

1. Initial condition
2. Final condition

ACKNOWLEDGMENT

The authors wish to acknowledge the department of mechanical engineering, Gyan Ganga Institute of Technology and Sciences, Jabalpur, India for their permission to conduct the experiments in their labs related to this research work.

REFERENCES

[1] Chitkara, N. R. and Bhutta, M. A. 'Dynamic heading of triangular, hexagonal, and octagonal shaped heads at high impact velocities': International Journal Advanced Manufacturing Technology, Vol. 18 pp. 332- 347, Springer-Verlag London Limited. 2001.
[2] Deryagin, B.V., 'What is Friction?' Izd Akad Nauk, USSR, Moscow, 1952
[3] Cull, G.W. 'Mechanical and metallurgical properties of powder forging'. Powder Metallurgy, Vol. 13, no 26, p 156, 1970.
[4] Rooks, B.W. 'The effect of die temperature on metal flow and die wear during high speed hot forging', 15 the Int MTDR Conf, p 487, 1974.
[5] Tabata, T. and Masaki, M. 'A yield criterion for porous metals and analysis of axial compression of porous discs', Memories of Osaka Institute of Technology, Series-B. Science and Technology. Vol.22, No. 2 p.45, 1978.
[6] Jha, A.K., and Kumar, S. 'Deformation characteristics and fracture mechanism during the cold forging of metal powder preform'. Int. J. Mech. Tool Des. Res. Vol.26, No.4, P 369, 1988.
[7] Singh, S. and Jha, A.K. 'Analysis of dynamic effects during high speed forging of sintered preforms', Journal of Materials Processing Technology, Elsevier, Vol. 112 pp. 53, 2001.
[8] Ranjan R. K. and Kumar S. 'High speed forging of solid powder polygonal discs with bulging', Tamkang Journal of Science and Engineering, Vol. 7, No. 4, pp 219-226, 2004.
[9] Ranjan R.K. and Kumar S. 'An upper bound solution for closed die sinter forging of hexagonal shapes', S¯adhan¯a , June, Vol. 29, Part 3, , pp. 263–273. © Printed in India, 2004.
[10] Sumathi, M. and Selvakumar, N. 'An investigation on the workability of sintered copper-silicon carbide preforms during cold axial upsetting'. Indian Journal of Engineering & Materials Sciences, April Vol. 19, pp 121-128, 2012.
[11] Verma D, Chandrasekhar P., Singh S. and Kar S. 'Investigations into deformation characteristics during open-die forging of SiCp reinforced aluminum metal matrix composites'. Journal of Powder Technology, 14 pp, Article ID 183713, Research Article, Hindawi Publishing Corporation, 2013.
[12] Jain S., Ranjan R.K. and Kumar S. 'Polygonal porous aluminum-copper composites cold forging at different strain rates', International Journal of Material Sciences and Manufacturing Engineering, January , Vol. 1, pp 1-10, ISSN: 2051-6851 © RECENT SCIENCE PUBLICATIONS ARCHIVES, 2015.

BIOGRAPHIES

Dr. Shrikant Jain received his degrees of B.E. (Hon's) Mech. Eng. form Government Engineering College Jabalpur (M.P.) India in 1970; and M.E. (Aeronautical Eng.) 1972-74 form Indian Institute of Science, Bangalore, India. He served as Senior Scientific officer II in Defense Research & Development Lab. Hyderabad (A.P.) India form 1974-76. In 1977 he established a production and processing unit at Jabalpur to cater the needs of defense establishments and public. Form 2004 he also became a faculty and presently he is Professor in the department of Mechanical Engineering at Gyan Ganga Institute of Technology and Sciences, Jabalpur (M.P.). He has been recently (2015) awarded PhD in the area of metallic composite forming form GLA University, Mathura (U.P.).

IARJSET

ISSN (Online) 2393-8021
ISSN (Print) 2394-1588

International Advanced Research Journal in Science, Engineering and Technology

SITES

Smart And Innovative Technologies In Engineering And Sciences

Gyan Ganga College of Technology

Vol. 3, Special Issue 4, November 2016

Dr. R. K. Ranjan received his degrees of M. Tech. in Production specialization from Institute of Technology, BHU, Varanasi, (U.P.) India, in 1997 and Ph.D. in Metal Powder Forming from Birla Institute of Technology, Messara (Jharkhand) India in 2005. At present he is Principal & Prof. at Gyan Ganga Institute of Technology & Sciences, Jabalpur, India. His area of interest is Metal Powder Forming. There are more than 50 research papers in his credit. He has completed one research project sponsored by Dept. of Science and Technology, India. Two Projects funded by AICTE, New Delhi, India are going on under his supervision.

Prof. Dr. Surendra Kumar received his degrees of B.Sc (Science group) from Punjab University in 1963, B.E. (Mechanical Engineering) form University of Allahabad in 1967, M.E., (Design and Prod. Of Machinery) from University of Allahabad in 1969 and PhD from Birla Institute of Technology (Ranchi University) in 1975. He has Professional Experience of 45 Years in the area of teaching & research. His Academic Achievement and Awards are: Outstanding research paper award, Institution of Engineers (I), 1984, including a Gold Medal and Many other academic/professional prizes. His Membership of Professional Societies are Member/fellow/ chairman of many academic and professional bodies such as Tribological Society of India, Institution of Engineers (I), Indian Society of Value Engineering, Indian Institute of Production Engineers, European Association of Material Forming and Institute of Metals etc. He holds University Level Responsibilities such as Dean Research & Development (to co-ordinate R&D activities including Ph.D. related work at university level). He Attended: International Conference – 20, National Conference – 30, Organized – 20. Number of Research Papers and Chapter in Book Published: Journals–108 (Published), International Conference–62 (Published), National Conference–88 (Published), Books – 10